Research Article GU J Sci, Part A, 12(1): 1-14 (2025) 10.54287/gujsa.1620831

Gazi University
Journal of Science
PART A: ENGINEERING AND INNOVATION
http://dergipark.org.tr/gujsa

Using Mine Waste and Bentonite in Cement for Enhanced Gamma Radiation Shielding

Setenay TUNÇKILIÇ[1] Ayşe Nur ESEN[1*]

[1] *Istanbul Technical University, Istanbul, Türkiye*

Keywords

Mine Waste Mud

Cement

Gamma-Ray

Linear Attenuation Coefficient

Shielding

Abstract

The increasing waste produced by the mining industry presents serious environmental challenges. This research focused on developing a sustainable material with enhanced shielding properties against gamma radiation by combining mine waste, which is rich in aluminum and iron, with bentonite and cement. We investigated the gamma-ray shielding properties of the shielding materials at energies of 59.54 keV, 661.66 keV, and 1115.54 keV using both experimental methods and theoretical approaches via EpiXS software. We calculated various metrics, including the linear attenuation coefficient, HVL, TVL, and radiation protection efficiency values. The findings revealed that a shielding material containing 55 wt.% cement and 17 wt.% mine waste mud could effectively reduce the intensity of low-energy gamma-ray photons by half with a thickness of less than 1 cm. The results indicate that incorporating mine waste significantly enhances radiation attenuation at lower gamma-ray energies and presents a promising opportunity for producing eco-friendly building materials, aligning with the principles of green engineering. Overall, using industrial waste in construction is cost-effective, providing long-term savings and environmental benefits.

Cite

Tunçkılıç, S., & Esen, A. E. (2025). Using Mine Waste and Bentonite in Cement for Enhanced Gamma Radiation Shielding. *GU J Sci, Part A*, *12*(1), 1-14. doi:10.54287/gujsa.1620831

Author ID (ORCID Number)	
0009-0008-1539-132X	Setenay TUNÇKILIÇ
0000-0003-4211-7728	Ayşe Nur ESEN

Article Process	
Submission Date	15.01.2025
Revision Date	13.02.2025
Accepted Date	28.02.2025
Published Date	26.03.2025

1. INTRODUCTION

Radiation shielding refers to the use of barriers to minimize exposure between a radiation source and the human body. The main mechanisms through which gamma rays interact include photoelectric absorption, Compton scattering, and pair production. For low-energy gamma rays, photoelectric absorption is most effective when high atomic number materials, like lead, are used. On the other hand, Compton scattering is effective with low atomic number materials such as aluminum and iron at higher energy levels. It's important to note that pair production only takes place with high-energy gamma rays, specifically those exceeding 1022 keV.

Cement is a non-metallic, inorganic material known for its hydraulic binding characteristics. When combined with water, it creates a paste that solidifies as hydrates develop. Once it hardens, the cement keeps its strength (Worrell, 2004). Cement-based materials for radiation shielding are popular due to their low cost and ability to be easily processed and shaped as needed. Shielding properties of concrete produced with different additives such as ilmenite and magnetite (Heniegal et al., 2022), hematite (Singh and Singh, 2021), waste glass (Eid et

*Corresponding Author, e-mail: anesen@itu.edu.tr

al., 2022), and steel slag (Baalamurugan et al., 2021) showed promising results. Bentonite is a type of absorbent swelling clay consisting mainly of montmorillonite, which can be categorized as Na-montmorillonite or Ca-montmorillonite. It finds applications in multiple areas, including industry, agriculture, mining, and engineering geology. Moreover, bentonite is frequently used to improve the effectiveness of cement mortars (Liu et al., 2020). Because of its swelling characteristics and non-toxic nature, bentonite can be incorporated into mortar to fill small voids within the cement matrix. This incorporation reduces water movement within the pore structure, enhancing waterproofing and impermeability. Recent studies have demonstrated the gamma-ray shielding capacities of bentonite, which serves as a suitable buffer and filler material for deep underground repositories in nuclear waste disposal (El-Khatib et al., 2021; El-Samrah et al., 2023; Sallem et al., 2022).

In recent years, the production of waste materials has increased, driven by the growing global population, advances in industry and technology, and heightened levels of consumption. The mining industry generates about 100 billion tons of waste annually (Vuillier, 2021). These pose persistent environmental and safety hazards. Recycling industrial waste into value-added functional materials is a sustainable way of industrial waste management (Saraee and Baferani, 2018; Xia et al., 2024). Green cement is an environmentally friendly cement that uses a carbon-negative production process. The primary raw materials used to produce green cement mainly include waste from industry (Wen et al., 2023). This reduces environmental impact and promotes sustainability. Incorporating waste as a partial replacement for raw materials in concrete production results in products with enhanced qualities, prevents waste from entering the environment, and decreases the need for extracting natural resources (Saraee and Baferani, 2018). In recent years, radiation shielding properties of mine wastes have also been investigated. Red mud, one of the most studied wastes, is a solid aluminum industrial waste that contains 30-60% hematite (Fe_2O_3), which is suitable for shielding high-energy X-ray and gamma rays (Liu et al., 2011). Shivani et al. (2024) researched red mud polymer composites as effective X-ray shielding materials, demonstrating that these composites effectively shield against X-rays. Arya et al. (2023) indicated that newly developed shielding materials created by incorporating barium hydroxide monohydrate and bismuth oxide into red mud are more economical for constructing radiation shielding materials than traditional materials like lead and concrete. Salati et al. (2021) showed that red mud addition to bentonite enhances the radiation shielding effectiveness of bentonite. Gili and Jecong (2023) studied the radiation shielding properties of various Philippine mine tailings and mining by-products, including ferronickel slag, nickel mine tailings, gold mine tailings, and copper mine tailings. Among the materials examined, nickel tailings were the most effective filler material for low-level radioactive waste, particularly in attenuating X-rays and gamma rays. Saraee and Baferani (2018) investigated the gamma radiation shielding properties of a material derived from lead-containing metallurgical solid waste by mixing cement and clay with the waste. Gallala et al. (2017) studied how adding barite-fluorspar mine waste as a fine aggregate affects the radiation-shielding properties of cement mortar. Their findings indicated that incorporating these mine waste aggregates enhanced the attenuation coefficient by 20%.

Incorporating industrial waste into construction materials provides both cost savings and environmental benefits. Construction costs can be significantly reduced by using these waste materials as alternatives to traditional options like cement and sand (Madhusudanan et al., 2016; Sharma and Kumar, 2024). This approach lessens the environmental impact of waste disposal and aids in conserving natural resources. Additionally, it decreases pollution and lowers greenhouse gas emissions (Cherian et al., 2022). In general, using industrial waste in construction materials is economically beneficial, leading to savings by lowering material expenses, alongside significant advantages for the environment.

The main goal of this research was to evaluate the effectiveness of gamma-ray shielding provided by cement-based materials that blend cement, bentonite, and mine waste mud rich in aluminum and iron. This study included experimental tests for gamma-ray transmission and theoretical calculations using EpiXS software. The results also aimed to demonstrate the potential for using industrial by-products to create more efficient and sustainable construction materials.

2. MATERIAL AND METHOD

2.1. Attenuation of Gamma-Ray

When a monoenergetic beam of photons interacts with a material, the number of photons that exit without interacting is calculated by Equation 1 (Tsoulfanidis and Landsberger, 2015).

$$I = I_0 \mathrm{e}^{-\mu x} \tag{1}$$

In the equation, I_0 is the initial gamma-ray intensity, I is the gamma-ray intensity after interacting with the material, μ is the linear attenuation coefficient (cm^{-1}), and x is the thickness of the material (cm). A high linear attenuation coefficient, which is the key indicator of a material's effectiveness as a shielding material, suggests that the material is effective at shielding. The mass attenuation coefficient of the material is calculated by dividing the linear attenuation coefficient by the material's density.

$$\mu_\rho = \frac{\mu}{\rho} \tag{2}$$

In the equation, μ_ρ is the mass attenuation coefficient ($cm^2\, g^{-1}$) and ρ is the material's density ($g\ cm^{-3}$).

Radiation protection efficiency (RPE) refers to the ratio of the radiation intensity measured before and after it interacts with a shielding material. It expresses how effective the material is at shielding ionizing radiation. The high RPE value indicates greater shielding of the radiation and, therefore, better radiation protection.

$$RPE(\%) = \left(1 - \frac{I}{I_0}\right) \times 100 \tag{3}$$

The half-value layer (HVL) indicates the thickness of material needed to reduce the initial radiation intensity by half, while the tenth-value layer (TVL) refers to the thickness required to reduce the same intensity to one-tenth. HVL and TVL are important metrics for evaluating how effectively a material can attenuate gamma radiation. The smaller these values, the more effective the material is at shielding against gamma radiation.

$$HVL = \frac{ln2}{\mu} \tag{4}$$

$$TVL = \frac{ln10}{\mu} \tag{5}$$

The measurement uncertainty was evaluated according to the Guide to the Expression of Uncertainty in Measurement (GUM) (JCGM, 2008) by considering all significant contributions. The combined standard uncertainties of the linear attenuation coefficient and radiation protection efficiency were calculated using Equations 6 and 7, respectively. Since both the half-value layer and the tenth-value layer values were derived from the linear attenuation coefficient, the uncertainty associated with the linear attenuation coefficient was also applied to each of them.

$$u_c(\mu) = \mu \times \sqrt{\left(\frac{u(I_0)}{I_0}\right)^2 + \left(\frac{u(I)}{I}\right)^2 + \left(\frac{u(x)}{x}\right)^2} \tag{6}$$

$$u_c(RPE) = RPE \times \sqrt{\left(\frac{u(I_0)}{I_0}\right)^2 + \left(\frac{u(I)}{I}\right)^2} \tag{7}$$

In the equation $u(I_0)$ and $u(I)$ are the standard uncertainties of the net photopeak count without and with shielding, respectively, and $u(x)$ is the standard uncertainty of the material thickness (Kahraman et al., 2024).

2.2. Preparation of Shielding Materials

CEM I 42.5R Portland Cement was used as the cement material in this study. Bentonite was obtained from Reşadiye, Tokat, and the mine waste mud was obtained from a mining company in Bursa province. According to the analysis conducted through X-ray fluorescence (XRF), the cement is predominantly composed of calcium oxide (CaO), while both bentonite and mine waste mud mainly contain silicon dioxide (SiO_2), as shown in Table 1. The chemical composition indicates that the bentonite is classified as Ca-bentonite, whereas the mine waste mud comprises approximately 32% aluminum oxide and 8% iron oxide.

Due to the moisture in the mine waste mud, it was left to dry in the sun for two days. Once it had dried, it was ground using an agate mortar and passed through an 850 µm sieve. As the cement and bentonite were already in powdered form, they were not processed with grinding or sieving. According to the TS EN 196-1 standard, the ratio of water to cement is 1:2 in the production technique of cement mixtures (Altuncı et al., 2022). All shielding materials were formulated from a composite of cement and water, employing a specific ratio of 25 grams of water to 50 grams of cement. The reference shielding material, designated as C, was comprised solely of cement and water. Additional shielding materials incorporated varying proportions of bentonite and mine waste mud, as outlined in Table 2. To assess the impact of bentonite and mine waste mud on the radiation shielding properties and facilitate comparison, a fixed quantity of 15 grams of each material was introduced individually into the cement and water mixture. Furthermore, 7.5 grams of bentonite and mine waste mud were introduced into the cement and water mixture while maintaining a total weight of 15 grams. The shielding material, which included cement, bentonite, and water, was prepared to evaluate the influence of bentonite and was referred to as CB. The mixture containing cement, mine waste mud, and water was developed to assess the effect of mine waste mud, denoted as CM. The shielding material, including cement, bentonite, mine waste mud, and water, was designated as CBM. Cement and water were initially blended to achieve a homogeneous mixture while preparing these shielding materials. Subsequently, bentonite and mine waste mud were incorporated, followed by thorough mixing to ensure uniformity throughout the composition.

Table 1. *Chemical compositions of materials (%)*

Component	Cement	Bentonite	Mine Waste Mud
SiO_2	5.39	65.02	48.08
Al_2O_3	6,91	21.60	31.61
Fe_2O_3	3.84	5.07	7.78
CaO	69.04	4.11	3.69
MgO	2.79	2.26	2.89
K_2O	-	0.54	2.48
TiO_2	-	-	1.04
ZnO	-	-	0.73
Na_2O	9.96	0.42	0.51

Table 2. *Composition of shielding materials by weight and their densities*

Shielding Materials	Code	Cement (%)	Bentonite (%)	Mine Waste Mud (%)	Water (%)	Density (g cm^{-3})
Cement	C	66.63	-	-	33.37	1.56
Cement and bentonite	CB	55.12	16.92	-	27.97	1.60
Cement and mine waste mud	CM	55.38	-	16.65	27.97	1.74
Cement, bentonite, and mine waste mud	CBM	55.45	8.30	8.35	27.90	1.67

Each mixture was divided into four equal pieces, placed in plastic molds, and allowed to dry (Figure 1). The pieces were kept for at least 30 days before experimental measurement. They were soaked daily until measurement to prevent crack development during this period. The masses and dimensions of the dried pieces were measured, and the experimental densities were calculated. Experimental densities varied from 1.56 to 1.74 g cm^{-3}. The shielding material with the highest density was the cement-mine waste mud blend (CM), while the lowest-density shielding material was the cement (C). The high density of the CM was attributed to its higher aluminum oxide and iron oxide content in mine waste mud than the other materials.

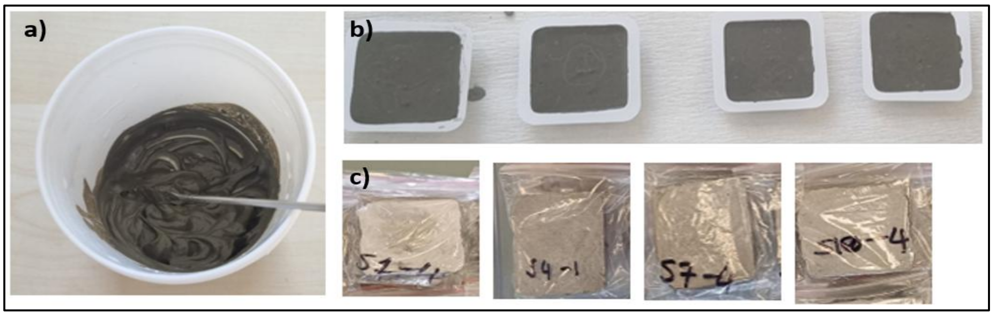

Figure 1. a) *Mixing,* ***b)*** *Shielding materials in the plastic molds, and* ***c)*** *Packing for measurement*

2.3. Gamma-Ray Shielding Measurements

The shielding experiments were performed using a NaI(Tl) scintillation detector (Alpha Spectra Inc. 3x3 inch). The detector was connected to a DigiBASE (ORTEC) digital gamma spectrometer with MAESTRO multichannel analyzer (MCA) software. To obtain a narrow beam geometry, the source was placed below the collimator, and the shielding material above the collimator. The collimator has a diameter of 7 cm, a length of 4.8 cm, and an internal cavity diameter of 1 cm. The measurement geometry was adjusted to match the shielding materials thickness and provide good counting statistics at the gamma-ray energy of interest in the spectrum in a short time (Figure 2). The uncertainties of the net photopeak count at the energy of interest in the spectra were less than 7%.

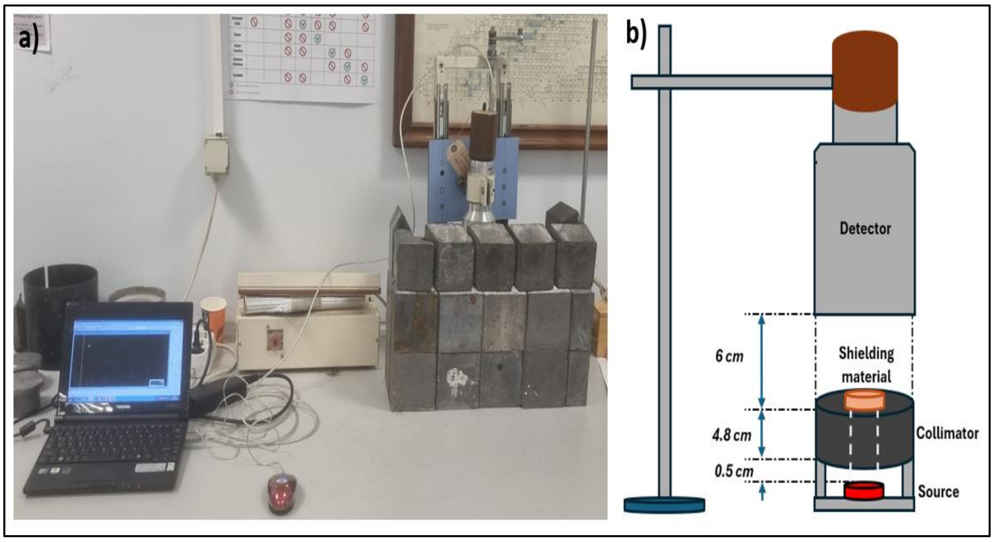

Figure 2. a) *Gamma spectrometer with NaI(Tl) detector,* ***b)*** *Measurement geometry*

^{241}Am, ^{137}Cs, and ^{65}Zn certified point sources were used in the experiments (Table 3). Thus, the gamma radiation shielding properties of the materials at low, medium, and high gamma-ray energies were investigated. The initial gamma-ray intensity of the sources (I_0) was measured without any shielding material present. To determine the gamma-ray intensity of the radiation after interacting with shielding material of different thicknesses (I), measurements were made by stacking four shielding materials on top of each other. The measured spectra were analyzed with the InterSpec spectral radiation analysis software developed by Sandia Labs (Johnson et al., 2021). The background spectrum was subtracted from the measured spectrum.

Table 3. *Properties of certified sources*

Radionuclide	Manufacturer	Energy (keV)	Certified Activity (kBq)	Reference Date
^{241}Am	Isotope Products Laboratories	59.54	36.21	01.12.2006
^{137}Cs	Czech Metrology Institute	661.66	17.58	30.06.2014
^{65}Zn	Czech Metrology Institute	1115.54	41.59	10.10.2023

2.4. EpiXS Calculations

The theoretical calculation of the linear attenuation coefficients was performed using EpiXS program (Hila et al., 2021). The input for the program consisted of the chemical compositions of cement, bentonite, mine waste mud, water (H_2O), and gamma-ray energies. The chemical compositions of cement, bentonite, and mine waste mud are given in Table 1. The program's output included these materials' total mass attenuation coefficients at 59.54 keV, 661.66 keV, and 1115.54 keV gamma-ray energies (Table 4).

Table 4. *The total mass attenuation coefficients ($cm^2\ g^{-1}$) of materials calculated by EpiXS*

Energy (keV)	Cement	Bentonite	Mine Waste Mud	Water
59.54	0.471	0.298	0.330	0.207
661.66	0.077	0.077	0.076	0.086
1115.54	0.060	0.060	0.060	0.067

The total mass attenuation coefficients obtained from the EpiXS program for cement, bentonite, mine waste mud, and water were multiplied by their respective weight percentages in the shielding material (Table 2). The results were then summed according to the content of the shielding material. The mass attenuation coefficient of the shielding material was multiplied by its density to calculate the linear attenuation coefficient of the shielding material.

3. RESULTS AND DISCUSSION

Figure 3 displays gamma-ray spectra at an energy of 661.7 keV, comparing measurements taken without any shielding material (represented by the black line) and with a 3 cm thick CM shielding material (represented by the green line). CM was selected because it demonstrated the best shielding properties among all the shielding materials. Both spectra were collected using the same measurement setup for 900 seconds. The uncertainties in the net photopeak counts were 1%. In addition to the photopeak of ^{137}Cs at 661.7 keV, the spectra also revealed the barium X-ray peak at 32 keV, which is part of the decay scheme of ^{137}Cs, as well as the lead X-ray peak in the 70-85 keV energy range due to the lead collimator. Additionally, the Compton continuum region was present in the spectra.

The difference in the height of the photopeaks at 661.7 keV in the spectra obtained with and without the shielding material reflects the difference in the photopeak counts. A higher photopeak observed without the shielding material indicates a greater count (I_0), while a lower photopeak with the shielding material signifies a reduced count (I). This suggests that the gamma-ray intensity was decreased due to the material's shielding effect.

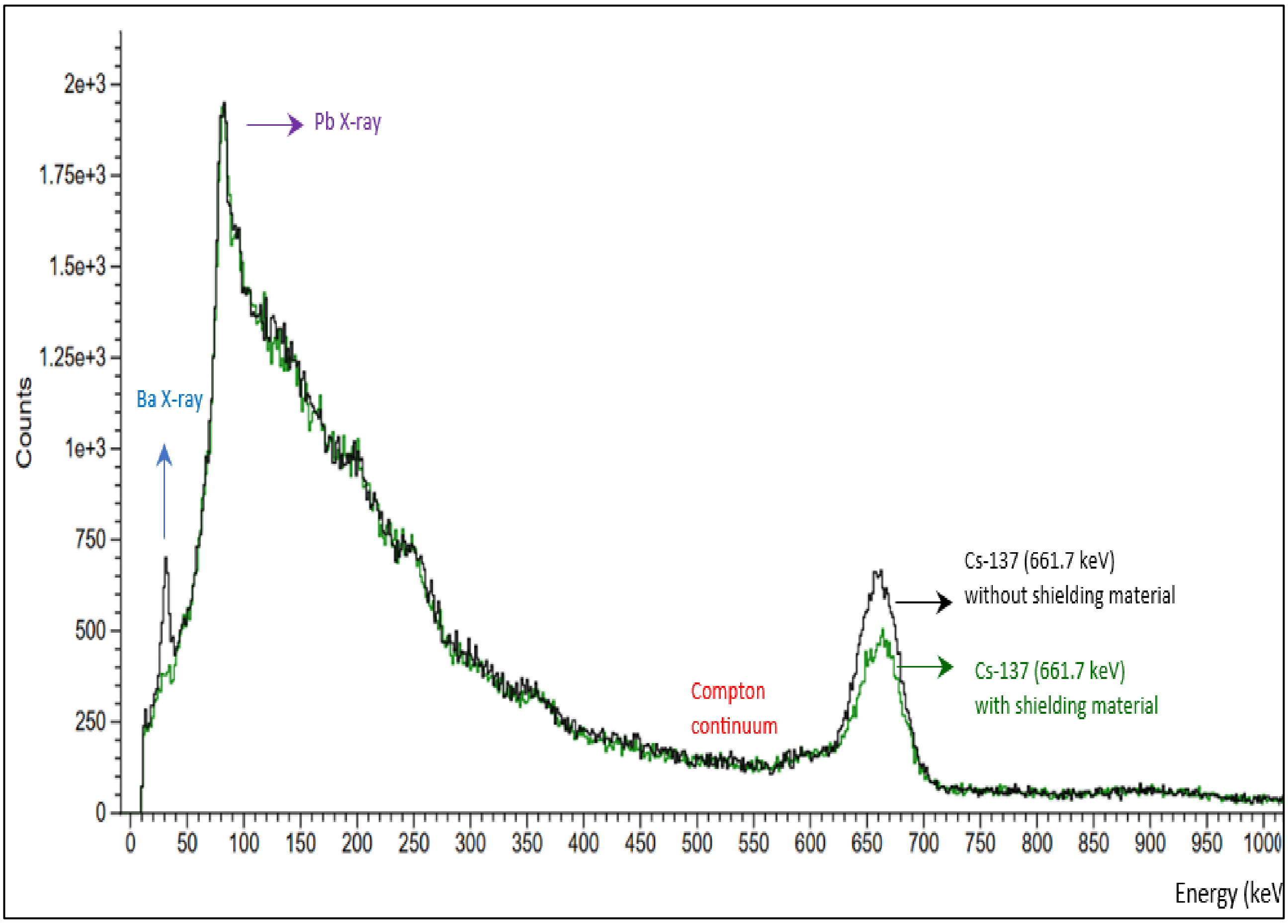

Figure 3. *Gamma-ray spectra of ^{137}Cs without shielding material and with 3 cm thick CM shielding material (counting time =900 s)*

I/I_0 ratios were calculated for shielding materials (C, CB, CM, CBM) of different thicknesses at gamma-ray energies of interest from the experimentally obtained spectra. The experimental linear attenuation coefficients of shielding materials were determined from the slope of the $\ln(I/I_0)$-x, and HVL, TVL, and RPE values were calculated. The combined standard uncertainty of the experimental linear attenuation coefficient, RPE, HVL, and TVL were given at k=1.

The experimental and theoretical linear attenuation coefficients of shielding materials are given in Table 5. For all shielding materials, the linear attenuation coefficient decreased as energy increased. According to the experimental results, the order of the linear attenuation coefficient from highest to lowest was CM > CBM > C > CB. The CM shielding material had the highest linear attenuation coefficient of all energies, and the CB shielding material had the lowest. According to the results obtained from EpiXS, CM exhibited the highest linear attenuation coefficients across all energies, similar to experimental results. The EPiXS results showed that the lowest linear attenuation coefficients were found for C and CB shielding materials, and the values were close. The results aligned with the chemical composition and density of the materials. CM, exhibiting the highest density, demonstrated the most significant gamma-ray attenuation across all energy levels. Conversely, the shielding materials with the lowest density, C and CB, consistently showed the lowest gamma-ray attenuation. When the shielding materials were compared according to the linear attenuation coefficients, it was observed that the shielding capability increased with the increase in the ratio of mine waste mud in the mixture. When shielding material C, containing only cement, and shielding material CB, consisting of the cement-bentonite mixture, are compared, it can be said that the addition of bentonite does not increase the gamma-ray shielding. When comparing experimental and EpiXS results, the differences range from 1% to 10%, indicating that the experimental and theoretical results are consistent. The differences arise from the uncertainties involved in shielding material preparation and gamma-ray measurement (Kahraman et al., 2024).

Table 5. *The linear attenuation coefficients (cm^{-1}) of shielding materials*

Energy (keV)	C			CB			CM			CBM		
	Exp. $\pm u_c$	EpiXS	Diff. (%)	Exp. $\pm u_c$	EpiXS	Diff. (%)	Exp. $\pm u_c$	EpiXS	Diff. (%)	Exp. $\pm u_c$	EpiXS	Diff. (%)
59.54	0.640 ± 0.024	0.598	7	0.613 ± 0.029	0.588	4	0.705 ± 0.037	0.650	8	0.673 ± 0.035	0.617	9
661.66	0.137 ± 0.002	0.125	10	0.116 ± 0.002	0.127	9	0.145 ± 0.002	0.138	5	0.138 ± 0.003	0.132	4
1115.54	0.096 ± 0.002	0.097	1	0.094 ± 0.002	0.099	5	0.105 ± 0.003	0.108	3	0.099 ± 0.004	0.103	4

The radiation protection efficiency values of CM shielding material are given in Figure 4. The RPE (%) values were calculated at varying shielding material thicknesses. The highest attenuation was noted at an energy of 59.54 keV; a 0.8 cm thick shielding material attenuated 43% of the incident radiation, while a 3 cm thick shielding material completely attenuated the low-energy gamma rays. The 3 cm shielding material at medium energy provided a 34% attenuation, while at high energy, it provided a 28% attenuation. The differences in RPE(%) values at the same thickness for medium and high energy were less pronounced than those observed at low energy.

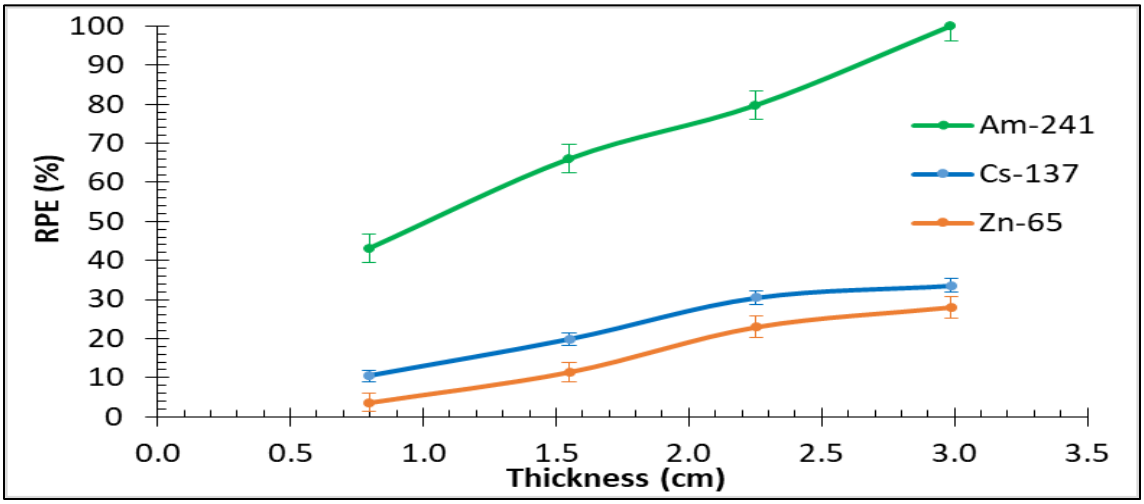

***Figure 4.** RPE (%) values of cement-mine waste mud (CM) shielding material*

Figure 5 shows the HVL and TVL of the shielding materials obtained from experiments. HVL values varied from 0.98 to 1.13 cm at 59.54 keV, 4.77 to 5.98 cm at 661.66 keV, and 6.61 to 7.35 cm at 1115.54 keV. TVL values ranged from 3.27 to 3.75 cm at 59.54 keV, 15.86 to 19.85 cm at 661.66 keV, and 21.95 to 24.42 cm at 1115.54 keV. For all energies, the order of HVL and TVL from lowest to highest is CM < CBM < C < CB. Smaller HVL and TVL values indicate a thinner and more effective shield.

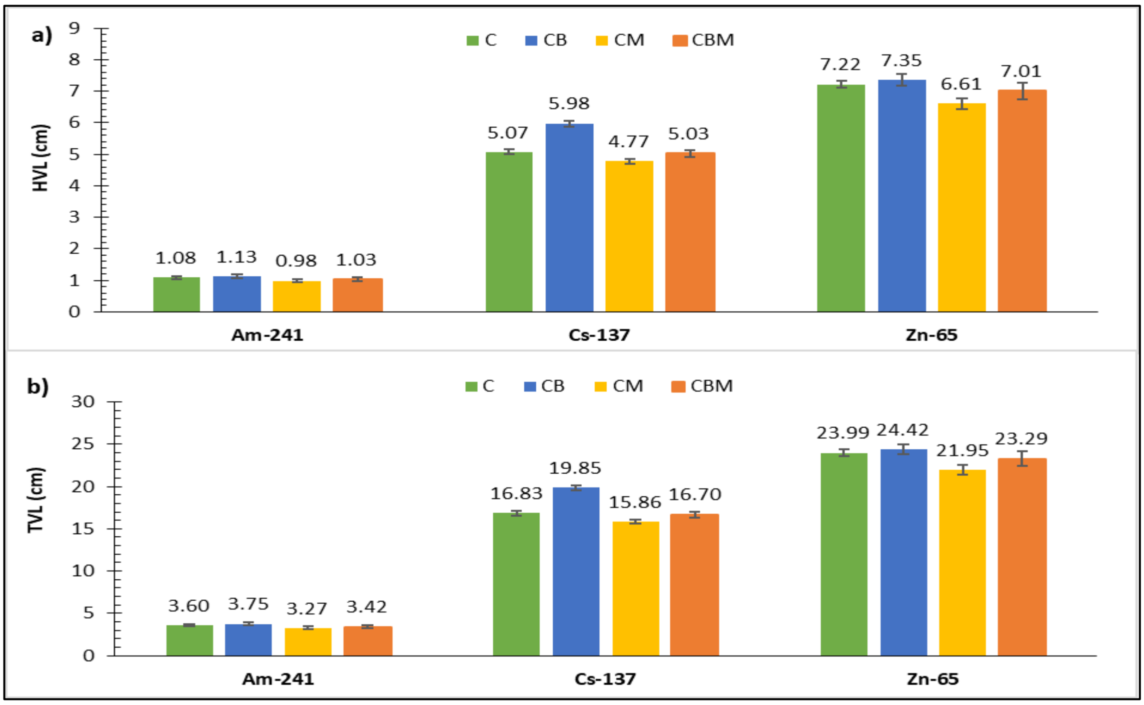

***Figure 5. a)** HVL, **b)** TVL values of shielding materials*

The HVL values obtained for the CM shielding material, which showed this study's best gamma ray shielding properties, were compared with selected studies where waste was used as radiation shielding material (Table 6). Compared to the cement mixture containing 40% silica waste in the study of Eid et al. (2022), it is seen that the HVL values obtained in our study were lower at 59.5 keV energy. Compared to barite-fluorspar mine waste in the study of Gallala et al. (2017) and copper mine tailing in the study of Gili and Jecong (2023), the HVL values obtained in our study were higher at 662 keV. This could be due to the higher density of copper used in the study of Gili and Jecong (2023), thus providing a higher shielding effect, and the higher weight percentage of mine waste in the study of Gallala et al. (2017) compared to aluminum and iron in our mine waste mud.

Table 6. *Comparison to other studies in the literature*

	Material	**Energy (keV)**	**HVL (cm)**
This study	Cement-Mine Waste Mud (17 wt.%)	59.5	0.98
		662	4.77
Eid et al. (2022)	Cement-Silica Waste (40 wt.%)	59.5	1.15
Gallala et al. (2017)	Barite-Fluorspar Mine Waste (30 wt.%)	662	4.62
Gili and Jecong (2023)	Copper Mine Tailings	662	3.22

4. CONCLUSION

There has been a growing search for alternative materials that can provide more cost-effective solutions to produce building materials in the construction industry. Utilizing waste not only helps reduce landfill accumulation but also conserves energy. By identifying the optimal amount of waste and replacing either aggregate or cement in concrete production, it is possible to achieve properties similar to ordinary concrete, thus offering solutions to the depletion of natural resources while simultaneously creating more economical and sustainable concrete.

This study investigated the gamma-ray shielding properties of composite materials made from a blend of cement, bentonite, and mine waste mud. To evaluate their effectiveness, shielding materials were prepared and subjected to experimental testing and theoretical analysis using EpiXS software at gamma-ray energies of 59.54 keV, 661.66 keV, and 1115.54 keV. The results showed that shielding material containing 55 wt.% cement and 17 wt.% mine waste mud could reduce the intensity of low-energy gamma-ray photons to half of its initial value when the thickness of the shielding material was less than 1 cm. In contrast, achieving a similar reduction for medium-energy photons required a greater shielding material thickness of approximately 4.8 cm. For high-energy photons, a thicker shielding material of about 6.6 cm was necessary for comparable attenuation. The findings indicate these materials exhibit strong shielding performance at lower gamma-ray energies. Consequently, concrete produced with mine waste additives containing metals is a highly effective candidate for nuclear applications, owing to its suitable nuclear radiation attenuation properties at low gamma energies.

AUTHOR CONTRIBUTIONS

Conceptualization, A.N.E; methodology, A.N.E.; software, S.T. and A.N.E.; title, A.N.E.; laboratory work, S.T. and A.N.E.; formal analysis, S.T. and A.N.E.; research, S.T. and A.N.E.; sources, A.N.E.; data curation, S.T. and A.N.E.; manuscript-original draft, S.T. and A.N.E.; visualization, S.T. and A.N.E.; supervision, A.N.E.; project management, A.N.E.; funding, A.N.E. All authors have read and legally accepted the final version of the article published in the journal.

ACKNOWLEDGEMENT

This research was supported by the Scientific Research Projects Department of Istanbul Technical University under Project Number MYL-2023-45205. We want to thank Research Assistant Deniz Agehan Kahraman for her assistance. Experimental studies were conducted at the Radioisotope Tracers and Applications Laboratory and the Radiation Detection and Measurement Laboratory at ITU Energy Institute.

CONFLICT OF INTEREST

The authors declare no conflict of interest.

REFERENCES

Altuncı, Y. T., & Öcal, C. (2022). TS EN 196-1 Standardında Belirtilen Üretim Tekniğinin İrdelenmesi. *Bitlis Eren Üniversitesi Fen Bilimleri Dergisi*, *11*(1), 21–28. https://doi.org/10.17798/bitlisfen.953562

Arya, R., Paulose, R., Agrawal, V., Pandey, A., Mishra, D., Kumar Sanghi, S., Akram Khan, M., Pada Mondal, D., Muhamed Shafeeq, M., Banerjee, K., Chatterjee, S., Mukhopadhyay, S., Roy, P., Ravishankar, R., Bhattacharya, C., Bhisikar, A., Mondi, P., Singh, U., Agnihotri, A., … Thankaraj Salammal, S. (2023). Next generation gamma ray shielding blocks developed using alumina industry waste. *Construction and Building Materials*, *373*. https://doi.org/10.1016/j.conbuildmat.2023.130895

Baalamurugan, J., Kumar, V. G., Chandrasekaran, S., Balasundar, S., Venkatraman, B., Padmapriya, R., & Raja, V. K. B. (2021). Recycling of steel slag aggregates for the development of high density concrete: Alternative & environment-friendly radiation shielding composite. *Composites Part B: Engineering, 216*. https://doi.org/10.1016/j.compositesb.2021.108885

Cherian, C., Siddiqua, S., Arnepalli, D.N. (2022). Utilization of Recycled Industrial Solid Wastes as Building Materials in Sustainable Construction. In: Reddy, K.R., Pancharathi, R.K., Reddy, N.G., Arukala, S.R. (Eds) *Advances in Sustainable Materials and Resilient Infrastructure. Springer Transactions in Civil and Environmental Engineering*. Springer, Singapore. https://doi.org/10.1007/978-981-16-9744-9_4

Eid, M. S., Bondouk, I. I., Saleh, H. M., Omar, K. M., Sayyed, M. I., El-Khatib, A. M., & Elsafi, M. (2022). Implementation of waste silicate glass into composition of ordinary cement for radiation shielding applications. *Nuclear Engineering and Technology*, *54*(4), 1456–1463. https://doi.org/10.1016/j.net.2021.10.007

El-Khatib, A. M., Elsafi, M., Almutiri, M. N., Mahmoud, R. M. M., Alzahrani, J. S., Sayyed, M. I., & Abbas, M. I. (2021). Enhancement of bentonite materials with cement for gamma-ray shielding capability. *Materials, 14*(16), 4697. https://doi.org/10.3390/ma14164697

El-Samrah, M. G., Tawfic, A. F., Sallam, F. H., & Omar, A. M. (2023). Investigation of specially designed bentonite samples as potential bricks with better radiation shielding properties. *Progress in Nuclear Energy*, *162*, 104778. https://doi.org/10.1016/j.pnucene.2023.104778

Gallala, W., Hayouni, Y., Gaied, M. E., Fusco, M., Alsaied, J., Bailey, K., & Bourham, M. (2017). Mechanical and radiation shielding properties of mortars with additive fine aggregate mine waste. *Annals of Nuclear Energy*, *101*, 600–606. https://doi.org/10.1016/j.anucene.2016.11.022

Gili, M. B. Z., & Jecong, J. F. M. (2023). The Potential Application of Mining Wastes and Slag as Radiation Shielding: A Characterization Study Using EpiXS. *Arabian Journal for Science and Engineering*, *50*, 3047–3058. https://doi.org/10.1007/s13369-023-07904-8

Heniegal, A. M., Amin, M., Nagib, S. H., Youssef, H., & Agwa, I. S. (2022). Effect of nano ferrosilicon and heavyweight fine aggregates on the properties and radiation shielding of ultra-high performance heavyweight concrete. *Case Studies in Construction Materials*, *17*, e01543. https://doi.org/10.1016/j.cscm.2022.e01543

Hila, F. C., Asuncion-Astronomo, A., Dingle, C. A. M., Jecong, J. F. M., Javier-Hila, A. M. V., Gili, M. B. Z., Balderas, C. V., Lopez, G. E. P., Guillermo, N. R. D., & Amorsolo, A. V. (2021). EpiXS: A Windows-based program for photon attenuation, dosimetry and shielding based on EPICS2017 (ENDF/B-VIII) and EPDL97 (ENDF/B-VI.8). *Radiation Physics and Chemistry*, *182*, 109331. https://doi.org/10.1016/j.radphyschem.2020.109331

JCGM. (2008). *Evaluation of measurement data-Guide to the expression of uncertainty in measurement (JCGM 100:2008)*. Joint Committee for Guides in Metrology.

Johnson, W., Chan, E., Walsh, E., Morte, C., & Lee, D. (2021). InterSpec v. 1.0.8. https://doi.org/10.11578/dc.20211202.6

Kahraman, D. A., Cogalmis, F. T., Esen, A. N., Haciyakupoglu, S., & Senkal, B. F. (2024). Neutron and gamma-ray shielding effectiveness of novel polyaniline composites. *Radiation Physics and Chemistry*, *219*, 111675. https://doi.org/10.1016/j.radphyschem.2024.111675

Liu, M., Hu, Y., Lai, Z., Yan, T., He, X., Wu, J., Lu, Z., & Lv, S. (2020). Influence of various bentonites on the mechanical properties and impermeability of cement mortars. *Construction and Building Materials*, *241*, 118015. https://doi.org/10.1016/j.conbuildmat.2020.118015

Liu, Y., Naidu, R., & Ming, H. (2011). Red mud as an amendment for pollutants in solid and liquid phases. *Geoderma*, *163(1–2)*, 1–12. https://doi.org/10.1016/j.geoderma.2011.04.00

Madhusudanan, S., & Amirtham, L. R. (2016). Optimization of construction cost using industrial wastes in alternative building material for walls. *Key Engineering Materials*, *692*, 1–8. https://doi.org/10.4028/www.scientific.net/kem.692.1

Salati, A., Share Isfahani, H., & Rowshanzamir, M. A. (2021). Evaluation of the performance of bentonite and red mud mixture as a shield in radioactive waste landfills. *Journal of Physics: Conference Series, 1973(1)*. https://doi.org/10.1088/1742-6596/1973/1/012200

Sallem, F. H., Sayyed, M. I., Aloraini, D. A., Almuqrin, A. H., & Mahmoud, K. A. (2022). Characterization and Gamma-ray Shielding Performance of Calcinated and Ball-Milled Calcinated Bentonite Clay Nanoparticles. *Crystals, 12(8)*, 1178. https://doi.org/10.3390/cryst12081178

Saraee, R. E. K., & Baferani, P. S. (2018). Application of Solid Waste Containing Lead for Gamma Ray Shielding Material. *Iranian Journal of Science and Technology, Transaction A: Science, 42(2)*, 941–946. https://doi.org/10.1007/s40995-016-0131-7

Sharma, K., & Kumar, A. (2024). Comparative Cost Analysis of Industrial Waste-Based Composite Materials Treated with Lime, Cement, and Alkali Activator in Comparison with Conventional Pavement Material. In: Agnihotri, A.K., Reddy, K.R., Bansal, A. (Eds), *Sustainable Materials. EGRWSE 2023. Lecture Notes in Civil Engineering, vol 509*, pp (149-157), Springer, Singapore. https://doi.org/10.1007/978-981-97-3153-4_11

Shivani, Vishwakarma, J., Dhand, C., M, M. S., Salammal, S. T., Gupta, G. K., Mishra, A., & Dwivedi, N. (2024). “Red-Mud, A Golden Waste for Radiation Shielding”: Red-Mud Polymer Composites for High-Performance Radiation-Shielding Components. *Journal of Hazardous Materials Advances*, *13*, 100394. https://doi.org/10.1016/j.hazadv.2023.100394

Singh, S., & Singh, K. (2021). On the use of green concrete composite as a nuclear radiation shielding material. *Progress in Nuclear Energy*, 136, 103730. https://doi.org/10.1016/j.pnucene.2021.103730

Tsoulfanidis, N., & Landsberger, S. (2015). *Measurement and Detection of Radiation (4th ed.).* CRC Press.

Vuillier, C. (2021). Future Of Mining With Zero Mine Waste | Knowledge Ridge. https://www.knowledgeridge.com/expert-views/future-of-mining-with-zero-mine-waste

Wen, J., Wang, B., Dai, Z., Shi, X., Jin, Z., Wang, H., & Jiang, X. (2023). New insights into the green cement composites with low carbon footprint: The role of biochar as cement additive/alternative. *Resources, Conservation and Recycling*, *197*, 107081. https://doi.org/10.1016/j.resconrec.2023.107081

Worrell, E. (2014). Cement and Energy, Reference Module. In: S. A. Elias (Ed.), *Reference Module in Earth Systems and Environmental Sciences* (pp. 307-315). Elsevier. https://doi.org/10.1016/B0-12-176480-X/00373-9

Xia, Y., Shi, D., Zhao, R., Yu, K., Liu, M., Mei, H., Xu, L., Zhao, Y., Wang, L., & Yan, J. (2024). Iron-rich industrial waste enhanced low-carbon radiation shielding functional composites. *Journal of Cleaner Production, 449*, 141649. https://doi.org/10.1016/j.jclepro.2024.141649